


**Please cite the Published Version**

Wortmann, FJ, Jones, C , Davies, TJ and Wortmann, G (2021) Perm-waved human hair: a thermorheologically complex shape memory composite. *Biophysical Journal*, 120 (17). pp. 3831-3840. ISSN 0006-3495

**DOI:** <https://doi.org/10.1016/j.bpj.2021.03.044>

**Publisher:** Biophysical Society

**Version:** Accepted Version

**Downloaded from:** <https://e-space.mmu.ac.uk/632054/>

**Usage rights:**  [Creative Commons: Attribution-Noncommercial-No Derivative Works 4.0](#)

**Additional Information:** This is an Author Accepted Manuscript of an article published in *Biophysical Journal*, by the Biophysical Society.

**Enquiries:**

If you have questions about this document, contact [openresearch@mmu.ac.uk](mailto:openresearch@mmu.ac.uk). Please include the URL of the record in e-space. If you believe that your, or a third party's rights have been compromised through this document please see our Take Down policy (available from <https://www.mmu.ac.uk/library/using-the-library/policies-and-guidelines>)

# **Perm-waved human hair: A thermo-rheologically complex, shape-memory composite.**

Franz J. Wortmann<sup>1\*</sup>, Celina Jones<sup>1</sup>, Thomas J Davies<sup>2</sup>, Gabriele Wortmann<sup>1</sup>

<sup>1</sup> Department of Materials, The University of Manchester, Manchester, UK

<sup>2</sup> School of Design, The University of Leeds, Leeds, UK

**Keywords:** human hair, permanent bending deformation, shape memory polymer, thermo-rheologically complex behaviour

\* Corresponding author:

Franz J Wortmann, Department of Materials, University of Manchester, Manchester M13 9PL, UK; E-mail: franz.wortmann@manchester.ac.uk

**ABSTRACT**

A ‘permanent’, bent shape can be imposed on a straight human hair by a two-stage reduction/oxidation (perm-waving) process. The process relies on the molecular level on sulfhydryl (SH)/ disulfide (SS) interchange as bond exchange reaction (BER). We expected a well-documented transition temperature around 60 °C to be the trigger for the shape memory (SM) –process of perm-waved hair. We confirm the existence of the SM-process as such and investigate its time- and temperature-dependence. The results show a two-stage SM-behaviour, implying two distinct variations of the BER. The model to fit the data contains two fractional, normalised, elastic bending rigidities, which are strictly compensatory. They show Arrhenius-type temperature dependence and a common activation energy of  $\approx -12$  kJ/mol. The characteristic relaxation time for the first SM-process shows little, if any temperature dependence ( $E_A = -4 \pm 2.7$  kJ/mol). This is in contrast to the second process ( $E_A = -58 \pm 5.5$  kJ/mol), but in line with the expected properties of the suggested BERs. None of the parameters shows any sign of the expected trigger transition ( $\approx 60$  °C). We hypothesize that this specific transition occurs only for large tensile deformations, when specific SS -bonds in the intermediate filaments of hair are activated. There is thus no specific ‘trigger’ transition for the SM of bent, perm-waved hair.

## **SIGNIFICANCE**

The term “permanent waving” describes the impartation of a stable bending deformation onto straight hair. Practical observations seem to suggest a lack of permanence. We investigate the time-dependent shape changes of permed hairs in water over a range of temperatures. We analyse the data on the basis of two viscoelastic shape memory processes, assuming two types of dynamic bond exchanges for the disulfide bonds in the hair proteins. We expected a transition around 60 °C to trigger shape memory. To our profound surprise no such transition could be found. This makes perm-waved hair an ‘atypical’ shape memory material. The results give interesting and novel insights into the complex structure/property-relationships for hair as a biological composite material.

## INTRODUCTION

Hair grooming practices frequently make use of hair shape changes, which may either be transient or perceived as permanent (1, 2).

In the first case, water and/or heat are applied to impart a non-permanent shape change to hair (straight  $\rightarrow$  curly; curly  $\rightarrow$  straight) by what is traditionally referred to as ‘cohesive’ set (3).

On a molecular basis, the process is dependent on the breaking and reformation of hydrogen bonds in the fibre/matrix structure of hair as a biological composite (2, 4). The recovery of the original form for cohesively set hair is a classic shape memory (SM) process. The process is controlled by the viscoelastic properties of hair (5, 6, 7, 8) and is triggered by its glass transition, which is highly dependent on water content (9, 10).

The term “permanent waving” describes the impartation of a stable bending deformation onto hair by a two-stage reduction/oxidation process. The corresponding treatment is the permanent straightening of naturally wavy hair. The imposition of this type of hair deformation is achieved by breaking/reducing disulfide (SS) bonds in the fibre under alkaline aqueous conditions, while it is deformed. The bonds are reformed through an oxidative treatment step while the hair remains in the deformed state (2, 11). The underlying bond exchange reaction (BER), that is the process of the relocation of the covalent bonds in equilibrium with the new form of hair, is referred to a sulfhydryl/disulfide (SH/SS) –interchange (12). For this specific BER, a transition around 60 °C in water at neutral pH has been extensively reported (13, 14, 15, 16, 17, 18, 19).

We thus expected this transition to trigger hair shape recovery after permanent waving.

Apart from academic interest in the various SM-mechanisms of hair, the motivation for this study also came from practical observations. These suggest a lack of true permanence of the hair style, perceived as a considerable loss of curliness over time.

Once we had confirmed the existence of the SM-process as such, it was our objective to develop a model-based systematization of the viscoelastic processes underlying the shape memory (recovery) of perm-waved hair in water. Our approach incorporates the principles of hair structure (2, 20, 21) and concepts for shape memory polymers (SMPs) (22, 23). A special focus is on various aspects of polymer viscoelasticity (24) and on the behaviour of thermorheologically complex materials (25, 26, 27). Our considerations benefitted from research on hydro-thermally activated, dynamic covalent networks of ‘smart’ bonds (28, 29) in shape memory polymers.

## **MATERIALS AND METHODS**

### **Sample Preparation**

Hair loops were treated on a cylindrical roller and then cut to measure the remaining bending deformation. This is a convenient measure of the efficiency of a permanent or non-permanent waving treatment with a close proximity to the practical situation (8, 30, 31, 32).

All experiments were performed on a commercial sample of untreated, mixed, Caucasian, medium brown hair, obtained in the form of flat tresses (approx. 1g/cm; Fa.Kerling, Backnang, Germany).

To determine bending recovery, a hair of approximately 20 cm length was taken at random from a tress. It was wound around a 12mm PVC-cylinder under a constant load of 200 mg and fixed at both ends with drops of nail polish. Care was taken to wind the hairs such that their axis was normal to the cylinder axis. Due to the ratio of hair vs cylinder diameter (max 100  $\mu\text{m}$  vs 12 mm), shear strains in the fibre are well below the limits of linear viscoelasticity ( $< 1\%$ ) (10, 32). The cylinder was then immersed in water for 30 min (20°C) to allow complete stress relaxation. Permanent set was achieved by then suspending the cylinder in a beaker and applying the following treatment sequence (30, 31):

Reduction: 1M thioglycolic acid (TGA), pH 9, 20 min, 20°C

1.Rinse: continuous exchange of demineralized water, 20 min, 20°C

Reoxidation: 2.3% H<sub>2</sub>O<sub>2</sub>, pH 7, 20 min

2.Rinse: continuous exchange of demineralized water, 20 min, 20°C

After the final rinsing step, the cylinder was removed from the beaker. The hair loops were cut without delay to yield partially opened hair rings. These were collected, dried under ambient conditions and combined into a “hair pool” of ultimately about 200 specimens. The pool of specimens was stored under ambient room conditions (approx. 55%rh, 22°C) for further use. It was assumed that under these conditions, where hair is well below its glass transition (10), no further change to the chemical fibre state would occur at least not in the time window of their use (33, 34). Fibre rings were used within a time window of one week to one month, so that experiments were done at times well removed from the treatment stage.

### **Measurements of Bending Recovery**

We determined the time-dependent opening (recovery) of groups of hair loops (30, 31) in water for temperatures between 35 °C and 95 °C. This temperature range includes the expected transition around 60 °C. The shape memory process was expected to be fast enough to be observable on an experimentally viable time scale (35).

For the experiments, five hair rings were taken at random from the fibre pool and dropped into a petri glass dish with demineralized water at room temperature and left to equilibrate for 30 min. This time was considered as sufficient to relax any ‘non-permanent’ viscoelastic processes related to the hydrogen bonds in hair (cohesive set) (8, 35). After this period, the loops were removed from the dish and directly dropped into a double-walled, thermostated glass dish with a flat bottom, containing water at temperatures between 35°C and 95°C.

The diameters of the partially opened loops were determined by taking calibrated images at seventeen predetermined and convenient times for up to 480 min. The readings were spaced roughly equally on the log-time scale. The first image was taken after  $\approx 15$  s, which was considered as adequate for temperature equilibration for the hair fibres. Since 15 s is short compared to the next reading at 120 s, the initial recovery readings were defined as effectively taken at  $t = 0$ . The lowest temperature (35 °C) was chosen to be well above the usual fluctuations of room temperature in a laboratory, so that a stable temperature could be maintained by heating alone.

Tests with sets of five hair rings were conducted in duplicates. For each experiment, data at a given time point were combined as means. This was an experimental necessity since due to intermittent image taking, individual fibre loops in a set could not be reliably traced over the experimental time range. However, this turned out to be only a minor problem, since differences between recovery values for duplicate tests were consistently  $< 0.02$  for all time points.

Time-dependent recovery  $R_{ec}(t)$  of a group of hairs is given by (30, 31, 32) :

$$R_{ec}(t) = 1 - D/d(t) \quad (1)$$

where  $D$  is the diameter of the cylinder, on which the fibres were treated.  $d(t)$  is the time-dependent mean diameter of the circles defined by the shapes of the partially opened fibre rings (see inset in Figure 1a).  $d(0)$  is the initial reading of the experiment at around 15 s. When  $R_{ec} > 0.5$ , the ring length covers less than half of the circumference of the circle it defines. In this case, the distance between the ring ends is taken as the length of an arc of the circle from which diameter readings were calculated. Figures 1a and b summarize the results.



### **Development of a Model Equation for the Description of Shape Memory / Recovery**

We base our approach on the well-documented morphological structure of hair as a biological, high-performance, fibre/matrix composite (4, 17, 18, 20). Intermediate filaments (IFs) in the core (cortex) of hair are aligned with the fibre axis and embedded in a matrix of IF-associated, amorphous proteins. This is the conventional, mechanical two-phase model for keratins, as shown in the inset of Figure 1b (2, 3, 8, 21).

Central to our approach is the assumption of a general analogy between shape memory from non-permanent, cohesive and from permanent bending deformation (36, 37). During permanent waving a hair is bent. The bending moment of the initially straight hair is relaxed under alkaline condition through reduction of about 20% - 40% of the cross-links (12, 38). These links are formed by the double-amino-acid cystine between and within protein chains. The highly reactive  $S^-$  -groups, resulting from the reduction, react with stressed disulfide bonds through sulfhydryl/disulfide (SH/SS) -interchange (14, 15). Through this BER, SS -bonds are broken and reformed in equilibrium with the bent configuration of the hair, thus stabilizing the perm-wave. Hair is thus an example for a biological composite with a clear link between dynamic bonds in its protein structure and a macroscopic response.

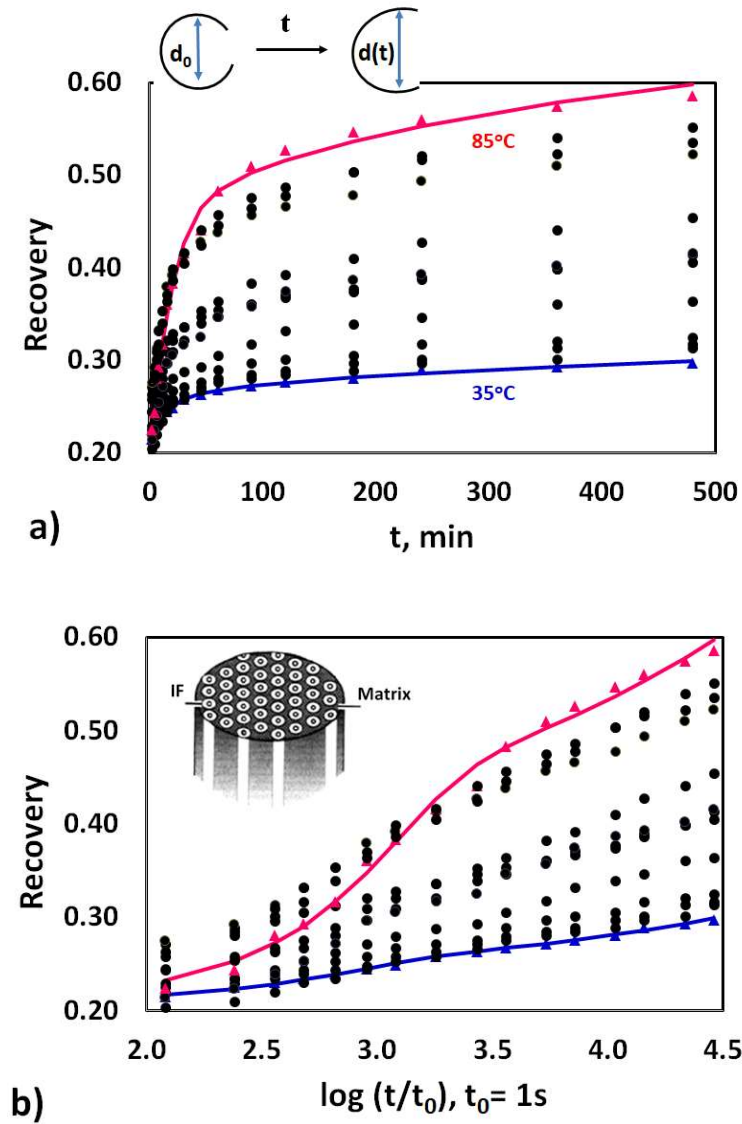
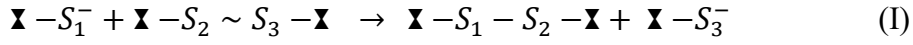


**FIGURE 1** a) Recovery values (means,  $N=5$ ) at the temperatures in the experimental range versus time (min). Lines through the lowest (35 °C) and the highest (85 °C) set of data are the fits according to Equation 9, using curve specific parameter values . Data sets are presented in 5 °C steps for the experimental temperature range. It just so happened that the data for 85 °C rather than 95 °C provided the highest final recovery values. The inset gives a description of the measurement of the hair loops. b) Data and fits as for a) but for the  $\log(t, s)$  –scale to highlight the specific structure of the curves. The inset gives a simple graphical representation of the IF/matrix composite structure in the cortex of hair (adapted from References 3, 4).

The description above is summarized in the chemical Eq. I:



The first part on the left hand side represents the free  $S_1^-$ -group formed under the alkaline conditions of reduction with thioglycollic acid (TGA, see Experimental above). The  $S_1^-$ -group is attached via a methylene group to a protein chain ( $\mathbf{X}$ —) and reacts with an unreduced, stressed disulphide bond ( $-S_2 \sim S_3-$ ). On the right hand side, an unstressed bond has formed ( $-S_1-S_2-$ ) and the free  $S_3^-$ -group is released. This group will then react with another stressed disulphide bond, in what is essentially an autocatalytic process. The new bent configuration of the hair is stabilized through the re-oxidation of about 70 – 80% of the  $SH$ -groups to form new cross-links (2, 30, 38). Upon releasing the hair from its constraints on the roller after reduction / reoxidation, it spontaneously opens to a new stable, bent state, which puts the newly formed  $SS'$ -bonds under stress.

As basis for the analysis of the recovery data, we suggest a fundamental analogy between the shape memory processes related to cohesive as well as permanent set. Against this background, the time-dependent recovery from permanent set,  $R_{ec}(t)$ , is assumed to be controlled by the general principles of linear viscoelasticity (5). The core principle is the interaction of the bending rigidities of the straight and the bent hair state according to Denby's equation, as an approximation of the Boltzmann Superposition Principle (6, 8, 24, 30, 32). We formulate Denby's (6) equation as (8, 30, 31):

$$R_{ec}(t) = B(t)/B(t-w) \quad (2)$$

$B(t)$  is the time-dependent bending rigidity of the initially straight hair, starting at  $t=0$ .  $B(t)$  is relaxed through the reduction process to a constant value  $B_{re}$ . The subscript relates to the reduction process.  $B_{re}$  remains unchanged under further processing, that is during rinsing and reoxidation (30, 31). It is thus the elastic stiffness, which remains unaffected by the chemical processes and is assumed to be equal for both the deformation and the recovery process.  $B(t-w)$  is the time dependent bending rigidity of the hair in its bent configuration after processing, when it is released at time  $w$ . At the time of release of a hair loop from the roller, that is at  $(t-w) = 0$ , the fibre shows the initial bending stiffness of the reoxidized hair  $B_{ro}$  (30). Setting  $w = 0$ , this yields for the time dependence of the overall recovery process:

$$R_{ec}(t) = B_{re} / B(t) \quad (3)$$

Eq. 3 implies the assumption of eventual total recovery ( $\lim_{t \rightarrow \infty} R_{ec}(t, T) = 1$ ). This is in line with the general behaviour of SMPs (39) and more specifically with observations for wool (40).

As a consequence of  $R_{ec}(t) \rightarrow 1$ ,  $B(t)$  will approach  $B_{re}$  as limiting elastic value.

On the basis of previous investigations (7, 8, 10), we formulate for  $B(t)$ :

$$B(t) = B_{re} + \Delta B \Psi(t) \quad (4)$$

In the context of the two-phase model for keratins,  $B_{re}$  is associated with the partly  $\alpha$ -helical, elastic, intermediate (IF) in hair (30, 31).  $\Delta B$  is the limiting, elastic bending rigidity of the matrix, and  $\Psi(t)$  is its relaxation function

Introducing Eq. 4 into Eq. 3 to fit the data showed that a single relaxation process (41, 42) is in fact insufficient to describe the sigmoid shape of the curves in Figure 1b. To approach this

problem, we found it plausible (35, 43, 44, 45), to expand Eq. 4 to contain two relaxation processes as:

$$B(t) = B_{re} + \Delta B_1 \Psi_1(t) + \Delta B_2 \Psi_2(t) \quad (5)$$

$\Delta B_1$ ,  $\Delta B_2$  are the fractional bending rigidities and  $\Psi_1(t)$ ,  $\Psi_2(t)$  the relaxation functions for the first and the second recovery process, accordingly.

Building on the suggested analogy between cohesive and permanent set, the relaxation functions are both *a priori*, but plausibly (8, 32) expected to conform to the well-known and widely used Kohlrausch-Williams-Watt (KWW) function (46, 47, 48, 49, 50) as:

$$\Psi(t) = \exp(-t/\tau)^m \quad (6)$$

where  $\tau$  is the characteristic relaxation time and  $m$  the related shape factor. These parameters control the position and the width of the relaxation function, namely, on the log-time scale (see Figure 1b). Combining Eqs. 5 and 6, we introduce  $\tau_1$  and  $\tau_2$  as the characteristic relaxation times for the two processes, while  $m_1$  and  $m_2$  are their individual shape factors.

Before combining the equations further, we introduce further normalizations as:

$$\Delta B_{n1} = \Delta B_1 / B_{re} \quad (7)$$

$$\Delta B_{n2} = \Delta B_2 / B_{re} \quad (8)$$

$\Delta B_{n1}$  and  $\Delta B_{n2}$  are the normalized fractional bending rigidities for each of the recovery processes. In what follows, these will be referred to as ‘bending intensities’.

Similar as tensile moduli (35, 51), bending rigidities (Equation 5) will be temperature dependent. This temperature dependence is expected (52) to be less for  $B_{re}$  as a property of the partly  $\alpha$ -helical IFs compared to  $\Delta B_1$  and  $\Delta B_2$  as properties of the largely (53), amorphous matrix. Also, temperature dependence is assumed for the characteristic relaxation times. In contrast,  $m$ -factors are both assumed as temperature-independent. This is in line with time/temperature superposition principles for polymers (24, 26) and analogous to the time/humidity superposition characteristics of keratins (7, 8).

This finally yields the time- and temperature-dependent recovery function  $R_{ec}(t, T)$  as basis to fit the data in Figure 1:

$$R_{ec}(t, T) = \frac{1}{1 + \Delta B_{n1}(T) \exp \left[ -\left( \frac{t}{\tau_1(T)} \right)^{m_1} \right] + \Delta B_{n2}(T) \exp \left[ -\left( \frac{t}{\tau_2(T)} \right)^{m_2} \right]} \quad (9)$$

Eq. 9 describes the shape memory of a very special case of a thermo-rheologically complex material (25, 27).

### Control of Data Overfitting

Eq. 9 contains an overall of six parameters, which ideally would be determined from the experimental data through a non-linear fit procedure. For this investigation Excel solver (Excel 2016, Microsoft) as well as Statistica (V13, Tibco Software Inc., 2017) were applied.

Due to the rather ‘simple’ shape of the curves in Figures 1a and b it was to be expected that substantial problems with overfitting would occur. This problem would be especially pronounced at low temperatures where contributions from the second, longer-term process were small. Working with the data, the problem of overfitting showed itself by large variations of parameter values, which were consistently associated with very high values for the

coefficient of determination ( $r^2 > 0.99$ ). Also, there were obvious compensation effects between  $\Delta B_{n1}$  -,  $\Delta B_{n2}$  - and  $m_1$  -,  $m_2$ -values.

For our final approach to data analysis on the basis of Eq. 9, we decided to introduce specific values for  $m_1$  and  $m_2$ . These were based on considerations of the specifics of the underlying SM-processes, as discussed below. By this, we succeeded to avoid compensations effects during curve fitting and improve precisions for both the relaxation times and the bending intensities.

There is a wealth of considerations in the literature on the nature of the KWW-function and on specific values of the shape parameter (48, 49, 50). In the current context, we found a paper by Pagnotta et al (54) especially helpful. They applied the KWW-function for dielectric data of the lysozyme/water system and modelled its glass transition as a percolation process. As limiting values for the shape of the KWW-function, they report  $m = 1$  at high and an extrapolated value of  $m = 0.35$  at low temperatures (54). For a completely different system, namely spin-glasses, Phillips (55) gives essentially the same temperature-dependent, limiting values of  $m = 1$  on the one hand and  $m \rightarrow 1/3$  ( $T \rightarrow T_g$ ) on the other. In spin-glasses, relaxation or rather magnetic re-organisation occurs through short-range exchange interactions. Such a process could be considered as an analogue to *SH/SS* -interchange. We find this correspondence interesting, remarkable and helpful.

Eq. 6 is a simple exponential, viscoelastic Debye process for  $m=1$ . It may also be viewed as a cumulative Weibull-distribution (cWD) function (56). Here  $m=1$  would signify that the failure rate, e.g. of bonds, is constant over time. Eq. 6 with  $m = 1$  also describes a classical chemical 1<sup>st</sup> order process, which proceeds at a rate that depends linearly on only one reactant concentration. A KWW-process with  $m = 1$  extends over about 2-3 decades on the log-time scale ( $t/\tau = 0.01$ ,  $\Psi = 0.99$ ;  $t/\tau = 10$ ,  $\Psi < 0.001$ ). Figure 2 shows such curves for  $\Delta B_{n1}(t)$  as well as for  $\Delta B_{n2}(t)$  for the limiting temperatures of the experimental range.

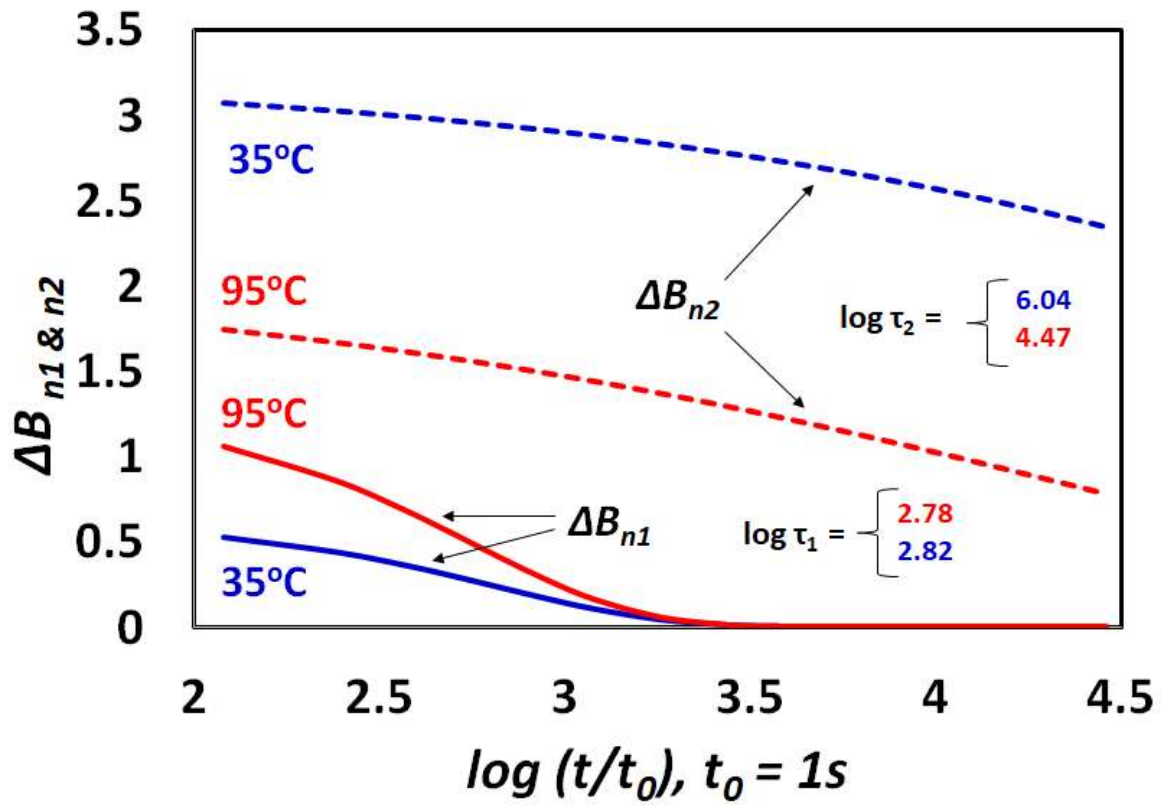


**FIGURE 2** The relaxation curves for the normalized bending intensities for the two viscoelastic contributions to matrix shape memory ( $\Delta B_{n1}$ ,  $\Delta B_{n2}$ ) against  $\log$  (time) (see Eq. 9). The curves for  $\Delta B_{n1}$  are the two lower and those for  $\Delta B_{n2}$  the two upper curves. The curves are based on fits of Eq. 9 to experimental data for 35 °C and 95 °C, using specific parameter values from Figures 4 and 5. Inflection points of the curves are given by  $\log(\tau_i)$  for which the colour-coded values are given on the graph.



Tobolsky (52) described a 1<sup>st</sup> order process for the stress relaxation in rubber at high temperatures. He associated the process with the cleavage of chemical bonds either along chains or at cross-links. The stress at any given point in time during the experiment is proportional to the number of cross-links still unbroken. In this context, he introduced the term ‘chemical’ relaxation.

The hypothesis of the stress-induced cleavage of polysulfide cross-links during rubber relaxation may be linked to the situation in reduced and re-oxidized hair (57). After re-oxidation and repeated rinsing, only about 70 – 80 % of  $S^-$ -groups, formed through reduction, will have reformed into  $SS$ -bonds (38). Under the more or less neutral pH after rising free  $SH$ -groups will remain in the hair. These are less reactive compared to the  $S^-$ -group for  $SH/SS$ -interchange (57).

For  $\Delta B_{nl}(t)$ , we propose the following molecular mechanism. Figure 3a shows the situation after spontaneous, initial recovery, where the free  $S_3H$ -group is left adjacent to two stressed  $SS$ -bonds. The following  $SH/SS$ -interchanges are driven by the fact that stressed  $SS$ -bonds have a lower activation energy than un-stressed bonds. If we assume that the free  $S_3H$ -group moves ‘downwards’ by pure chance, this will finally leave the  $S_6H$ -group, isolated from the remaining, stressed  $S_1S_2$ -bond (see Figure 3c). As long as sufficient numbers of  $SH$ -groups in the neighbourhood of stressed  $SS$ -bonds are present, the process may be expected to show a constant failure rate. This process may also be seen as an autocatalytic process (58) in the matrix proteins of hair. Whatever the model consideration for the process, the  $cWD/KWW$  function with  $m = 1$  would be a plausible analytical description. This suggestion is supported by the observation that relaxation of hair during reduction follows consistently the  $m=1$  kinetic pathway (11, 59).

Once the  $\Delta B_{n1}(t)$  - process has taken place, remaining free *SH*-groups and strained *SS* -bonds are far apart (see Figure 3c). They will only meet each other through extended chain movements in the wider structure of the matrix. These may be associated with a chain percolation / diffusion process or various other models for molecular movement, consistent with the *KWW*-function (48, 50, 60).

Pagnotta et al (54) and Philipps (55), for very diverse systems, found limiting lower values for  $m$  in Eq. 6, which are consistent with the ‘universal’ value of  $m \approx 1/3$  (49). This yields a relaxation function over about 6-7 decades of time. The value has been observed for or is consistent with the relaxation and creep curves for a wide variety of materials (49, 61, 62), including, metals, glasses, polymers, rubbers, bone (45) as well as keratins (7, 8).

Investigations on the recovery of human hair from cohesive set (8) have given an experimental value of  $m = 0.28 \pm 0.02$ . In view of the suggested analogy between the shape memory processes related to cohesive and permanent set, respectively, we have pragmatically chosen  $m_2 = 0.3$  to fit the  $\Delta B_{n2}(t)$  - process in Eq. 9. This appears reasonable when considering the range and the anticipated precision of the experimental and theoretical  $m$ -values (61). Figure 2 gives *KWW*/ $m=0.3$  -curves for  $\Delta B_{n2}(t, T)$  for the limiting temperatures of the experimental range.

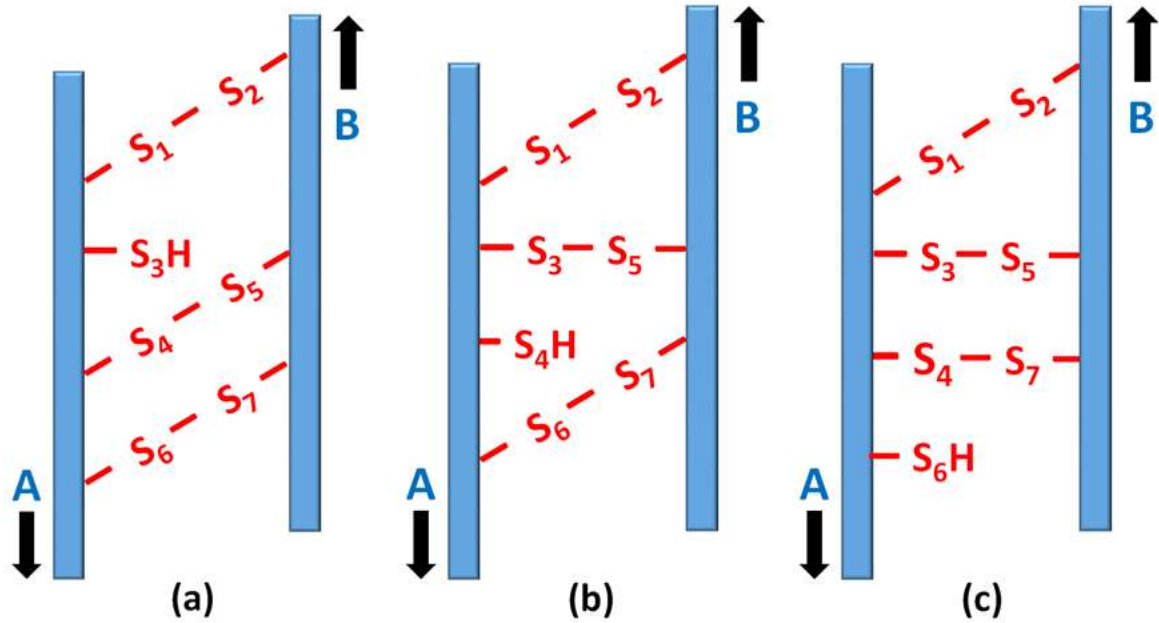


**FIGURE 3** Graphical representation of the state of the SS -bonds in the matrix during the shape memory processes after perm-waving (adapted from References 3, 11, 20). Two protein chains are considered, which are displaced (sheared) against each other (as indicated by the arrows) due to the interacting bending moments, according to Eq. 3. For graphical reasons shearing enables a more straightforward presentation of the mechanisms compared to bending.

a) After shearing upon release of the bent and perm-waved hair, the two protein chains in the matrix are linked through stressed disulphide bonds.  $S_3H$  represents a free sulfhydryl group, remaining in the fibre after processing. b) Rather than with the adjacent  $S_1S_2$  -bond, the group, by pure chance, is assumed to enter alternatively into an equivalent bond exchange reaction (BER) with the stressed  $S_4S_5$ -bond. This leads to the unstressed  $S_3S_5$ -bond and the free  $S_4H$ -group. c) This new group will then interact with the stressed  $S_6S_7$ -bond to form the unstressed  $S_4S_7$ -bond and the free  $S_6H$ -group. This group is now well removed from the remaining, stressed  $S_1S_2$  -bond.

## RESULTS

Figure 1a shows recovery vs time for selected temperatures to cover the experimental range. For all temperatures, an initial recovery of about 20% is followed by a rapid further increase, for which the extent increases with temperature. Beyond times of  $\approx 100 \text{ min}$  the curves appear to follow a slow, somewhat linear process, where slopes again increase with temperature. This is analogous to the characteristic behaviour of polymers under creep conditions (24). The maximum recovery, which was observed over the experimental time range and at the highest temperatures (85 °C - 95 °C), was  $\approx 55 \% - 60 \%$ .

To get a better view of the fine structure of the recovery process, Figure 1b realizes a plot of recovery against log (time) for the data sets. On the log(t)-scale, the recovery curves exhibit a non-symmetrical, sigmoid shape. The shape is rather faint at lower temperatures ( $< 60 \text{ °C}$ ), where it shows itself as an apparent linear increase but becomes increasingly obvious at higher temperatures ( $\approx 80 - 90 \text{ °C}$ ).

The start values of the curves in Figure 1b, that is the initial recoveries, are on the basis of Equation 2 given as:

$$R_{ec}(0) = B_{re}/B(0) \quad (10)$$

The analysis of the experimental  $R_{ec}(0)$ -values shows that, there is no significant dependence on temperature and a mean ( $\pm \text{SE}$ ) of  $0.225 \pm 0.0041$  is observed. This implies equal temperature dependencies for the parameters in Eq. 10, so that effects of the expected transition at around 60 °C would be compensated.

Figure 4 summarises the data for  $\Delta B_{n1}$  and  $\Delta B_{n2}$  versus temperature.  $\Delta B_{n1}$  increases and  $\Delta B_{n2}$  decreases essentially linearly in a strictly compensatory manner, as implicit in Eq. 9. For lower temperatures (35+ °C) the intensity of the first process is low and the second process clearly

dominates recovery, accordingly, with a ratio of about 6:1. At the high end of the experimental range (80+ °C), intensities become essentially equal for the two processes. There is no indication of the suggested transition for the BER at around 60 °C, related to *SH/SS* - interchange (14, 16, 19).

To investigate temperature dependence,  $\Delta B_{n1}$  – and  $\Delta B_{n2}$  - data are transformed, assuming Arrhenius-type behaviour:

$$\Delta B_n(T) = C \exp (-E_A/RT) \quad (11)$$

Plots of  $\ln(\Delta B_n)$  vs  $1/T$  show for both  $\Delta B_{n1}$  and  $\Delta B_{n2}$  good straight line fits with process specific intercepts of  $C$  and slopes of  $(-E_A/R)$ .  $E_A$  is the activation energy for the bending intensity and  $R$  the gas constant. The parameter values are given in Table 1. Due to the perceived graphical redundancy with respect to Figure 4, no graph is given for the Arrhenius relationships.

$\Delta B_{n1}$  increases and  $\Delta B_{n2}$  decreases with temperature, so that calculated activation energies, derived from the Arrhenius-plots, are positive (15 kJ/mol) and negative (-9 kJ/mol), respectively (see Table 1).

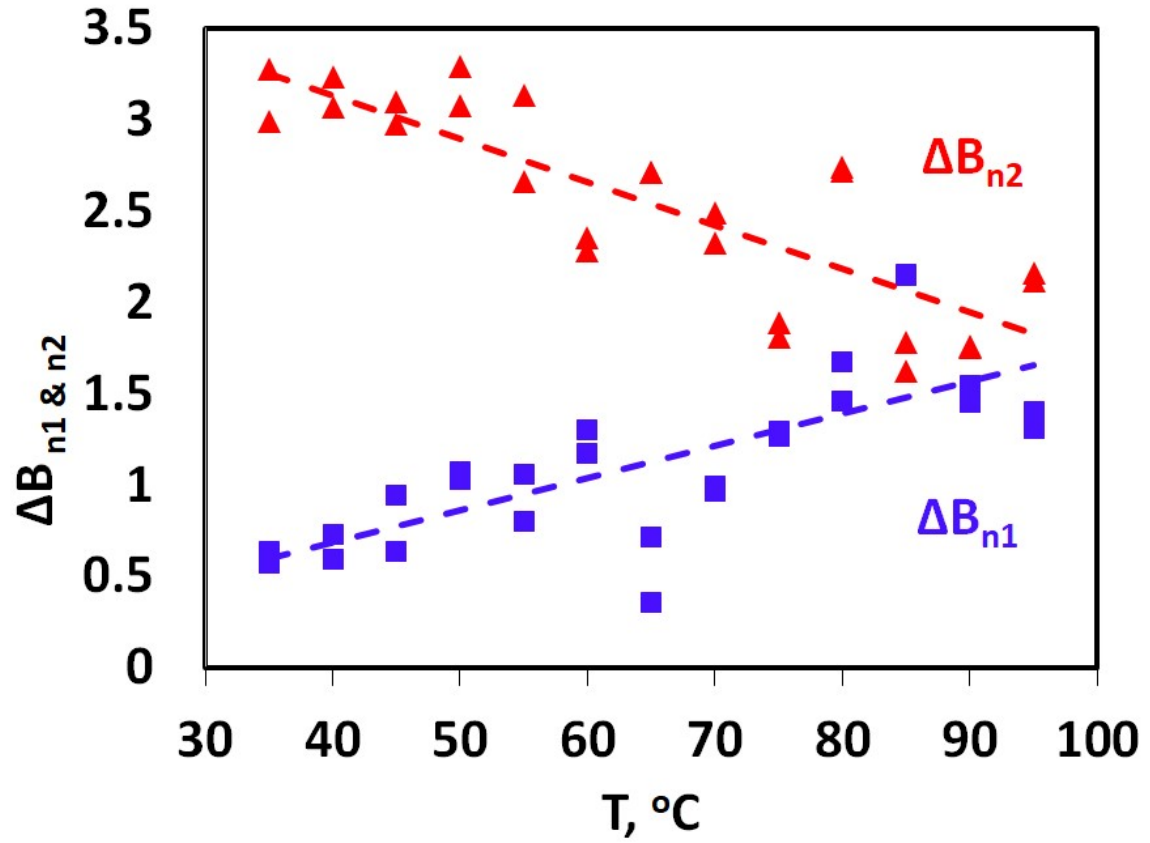


**FIGURE 4** Normalized intensities of partial bending intensities,  $\Delta B_{n1}$  and  $\Delta B_{n2}$  vs temperature, as indicated (see Eqs. 7 and 8). Regression lines through the data are given to highlight linearity.

**TABLE 1** Arrhenius-equation fits (see Eq. 11) for the parameters of Eq. 9.  $C$  = y-axis intercept,  $(-E_A/R)$  = slope,  $E_A$  = activation energy,  $SE$  = standard error,  $r^2$  = coefficient of determination. The data, underlying the fits, are graphically summarized in Figures 4 and 5. The slopes of the straight lines and thus the activation energies ( $E_A$ ) are highly significant on the 95%-level ( $p < 0.001$ ,  $N = 26$ ) for all cases, except for  $\ln \tau_I$  ( $p = 0.16$ ; set in *italics*).

Parameter	$C \pm SE$	$(-E_A/R) \pm SE$	$E_A \pm SE$ , kJ/mol	$r^2$
$\Delta B_{n1}$	$5.5 \pm 1.08$	$-1.8 \pm 0.36$	$15 \pm 3.0$	0.512
$\Delta B_{n2}$	$-2.4 \pm 0.47$	$1.1 \pm 0.16$	$-9 \pm 1.3$	0.664
$\ln \tau_1$	<i><math>5.1 \pm 0.97</math></i>	<i><math>0.5 \pm 0.33</math></i>	<i><math>-4 \pm 2.7</math></i>	<i>0.285</i>
$\ln \tau_2$	$-8.8 \pm 1.97$	$7.1 \pm 0.67$	$-59 \pm 5.5$	0.824

Figure 5 summarizes the data for the characteristic relaxation times of the two processes in an Arrhenius –plot as  $\ln \tau_i$  vs  $1/T$ . The slope of the straight line fit for  $\ln \tau_1$  is not significant on the 95%-confidence level ( $p = 0.16$ ) and the data conform to a mean ( $\pm$  SE,  $N=26$ ) of  $\ln \tau_1 = 6.48 \pm 0.055$ . In the given experimental context,  $\ln \tau_1$  is thus found to be effectively independent of temperature. This yields a characteristic relaxation time for the first, fast process of  $\approx 11$  min (652 s). The activation energy, which is formally calculated for  $\ln \tau_1$ , is very low and lacks precision with  $-4 \pm 2.7$  kJ/mol (see Table 1). The value is significantly different from zero only on the 84% confidence level.

The temperature dependence of the characteristic relaxation time for the second, slow process ( $\tau_2$ ) is quite pronounced, in contrast. It decreases significantly with temperature and essentially linearly in the Arrhenius plot. Within the experimental temperature limits,  $\tau_2$  varies between  $\sim 13$  days (35°C) and  $\sim 9$  hrs (95 °C). The fit in Figure 5 yields an activation energy of  $-58 \pm 5.5$  kJ/mol (see Table 1).



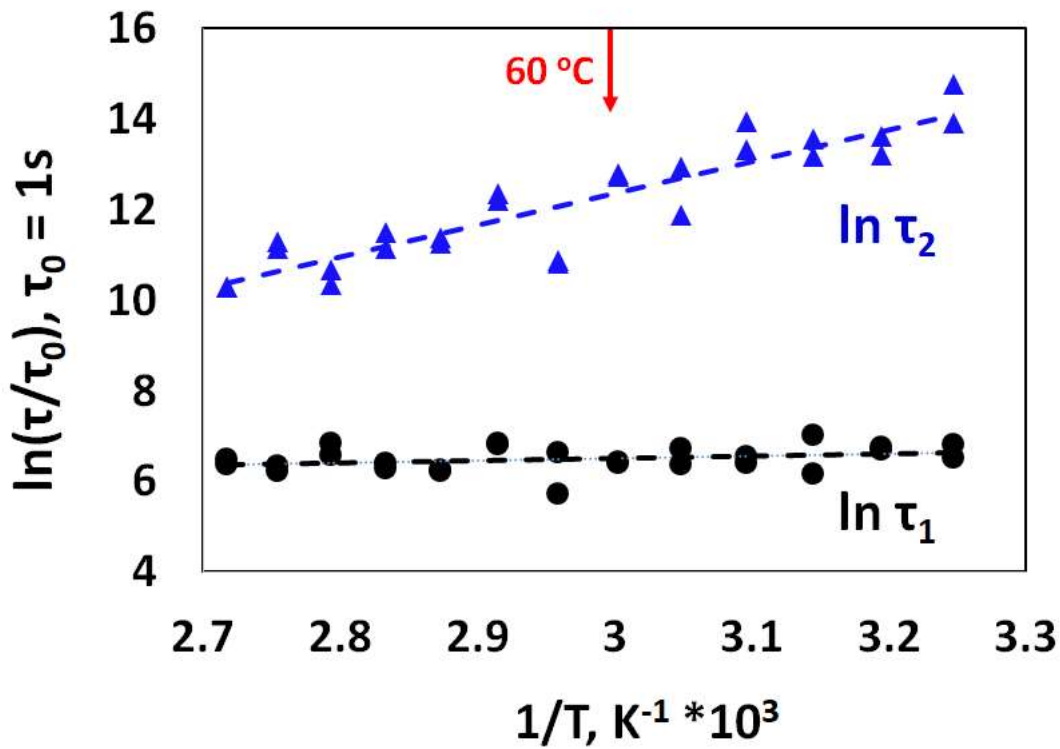


**FIGURE 5** Data for the characteristic relaxation times (s)  $\tau_1$  (●) and  $\tau_2$  (▲) in an Arrhenius plot as  $\ln(\tau_i)$  vs  $1/T$  (N=26). Straight lines are fitted through the data. The coefficients for the linear fit equations are given in Table 1. The position of the anticipated, but conspicuously absent transition around 60 °C is marked.

## DISCUSSION

### General Considerations

The recovery curves, which we observed in the range 35 – 95 °C in water, indicate a two-stage process of shape memory (see Figure 1b). It is interesting to note that the temperature above which the second process seems to become more apparent coincides with the expected transition temperature ( $\approx 60$  °C). Such a combination of a fast and slow process can be seen in the relaxation curves of wool in water (1°C – 90°C) (35). Namely, the 2<sup>nd</sup> process is suppressed at low pH (35), supporting the notion that the relaxation mechanism is related to *SH/SS*-interchange. The assumption of two relaxation processes is also broadly supported by the investigation by Wall et al (43) on multiple relaxations processes in hair.

The presumed analogy between cohesive and permanent set leads to the application of the Denby-equation. The analysis of the recovery curves is based on two independent and consecutive viscoelastic processes for which the relaxation functions are assumed to be of the KWW -type (8, 32, 48). To enable a stable fit of the data through Eq. 9 and against the background of general considerations (54, 55), we introduce specific shapes for the viscoelastic functions. We base these on the hypothesis of two different BER -mechanisms of *SH/SS* -interchange of stressed disulphide bonds. On this basis, we could successfully fit the overall shape memory / recovery curves and determine the temperature dependencies of the bending intensities  $\Delta B_{n1}$  and  $\Delta B_{n2}$  and of the characteristic relaxation times  $\tau_1$  and  $\tau_2$ .

## Bending Intensities

Over the experimental temperature range (35 – 95 °C)  $\Delta B_{n1}$  increases 2.8 -times while  $\Delta B_{n2}$  in parallel decreases to 0.56, assuming a linear fit and taking 35 °C as point of reference (see Figure 4). The relative changes are much larger than would be expected from the drop of modulus over the temperature range for wool and hair ( $\approx 20\%$  : 15, 35, 51).

The tensile modulus of wool and hair in water is mainly a property of the partly  $\alpha$ -helical IFs with a relatively small contribution by the amorphous protein matrix (3, 21, 63). The temperature dependencies of  $\Delta B_{n1}$  and  $\Delta B_{n2}$  imply in view of Eqs. 7 and 8 substantial temperature dependencies of the fractional bending rigidities  $\Delta B_1$  as well as of  $\Delta B_2$ , which are considered as properties of the amorphous matrix. Such significant changes of both bending intensities with temperature appear reasonable, since water has a strong plasticizing effect on the matrix (7, 10).

Given the strictly compensatory relationship between  $\Delta B_{n1}$  and  $\Delta B_{n2}$ , their activation energies have opposite signs. However, the difference between the absolute values for their  $E_A$ 's appears rather puzzling at first sight. Our explanation for this problem follows the following line of thought. The elastic tensile modulus of hair is essentially a property of the IFs. In water it decreases with temperature (51), consistent with an activation energy of  $E_A = -3.7 \pm 0.46 \approx -4$  kJ/mol. This is in good agreement with earlier results for wool (- 3.9 kJ/mol: 35). We assume this value to be a reasonable estimate for the activation energy of  $B_{re}$  [ $E_A(B_{re})$ ], as a property of the IFs. From Eqs. 7 and 8 and with the values in Table 1 it can be shown that:

$$E_A(\Delta B_1) = E_A(\Delta B_{n1}) + E_A(B_{re}) = 15 - 4 = 11 \text{ kJ/mol} \quad (12)$$

and

$$E_A(\Delta B_2) = E_A(\Delta B_{n2}) + E_A(B_{re}) = -9 - 4 = -13 \text{ kJ/mol} \quad (13)$$

In view of the underlying assumptions, the absolute values for the outcomes of Eqs. 12 and 13 are considered as being essentially equal at  $|E_A| \approx 12 \text{ kJ/mol}$ . As a condition inherent to Eq. 9, the partial bending rigidities thus show the same activation energies, though with opposite signs. They thus change in a consistent and truly compensatory manner. Since the opposite signs for the activation energies are imposed by the compensatory nature of Eq. 9 and since bending rigidities will decrease with temperature, we assign a ‘true’ activation energy of  $-12 \text{ kJ/mol}$  to both  $\Delta B_1$  and  $\Delta B_2$ .

The fractional bending rigidities  $\Delta B_1$  and  $\Delta B_2$  are associated with the amorphous matrix component. Accordingly, the result that their activation energy of  $\approx -12 \text{ kJ/mol}$  is about 3x higher than the estimate for  $E_A(B_{re})$  ( $\approx -4 \text{ kJ/mol}$ ), as a property of the partially crystalline IFs, appears reasonable. Due to the axially oriented filament/matrix structure of the hair fibre core (cortex), torsional properties are largely a property of the matrix (3). Feughelman and Mitchell (64) investigated the torsional modulus of wool fibres in water at temperatures between  $7^\circ\text{C}$  and  $44^\circ\text{C}$ . Their data conform to  $E_A = -16 \pm 2.2 \text{ kJ/mol}$ . This value in satisfactory agreement with the value of  $-12 \text{ kJ/mol}$ , as given above. This supports the underlying assumption of  $\Delta B_{1\&2}$  as being matrix properties.

We were surprised that the results for  $\Delta B_{n1 \& n2}(T)$  in Figure 4 show no indication of the expected transition around  $60^\circ\text{C}$  (17, 18, 19). Initially, we assigned this absence to possible thermal compensation effects in Eqs. 7 and 8. However, the differences between the activation energies for  $B_{re}$  and  $\Delta B_{1 \& 2}$  do not support this view but rather suggest the factual absence of the transition.

### Characteristic Relaxation Times

The characteristic relaxation time for the first SM-process ( $\tau_1$ ) is found to only show a very small and statistically non-significant dependence on temperature [ $E_A(\tau_1) = -4 \pm 2.7 \text{ kJ/mol}$ ]. It

is interesting to note, however, that Haly and Snaith (41) found a similarly low value ( $E_A = -0.65 \text{ kcal/mol} = -2.7 \text{ kJ/mol}$ ) for the 2<sup>nd</sup> stage of the recovery of wool fibres from tensile cohesive set. They consider this low value as being consistent with a bond exchange mechanism, for which the required energy is small. This corresponds to the mechanism which we propose for the first process of shape recovery, as discussed above. It also fits into the framework of the suggested formal analogy of shape memory / recovery processes for cohesive and permanent set. Though the accurate determination of the variation of  $\tau_1$  with temperature is thus somewhat beyond the resolution of our method,  $E_A(\tau_1) = -4 \text{ kJ/mol}$  appears to be a reasonable estimate in the context of the literature (41).

In contrast, the activation energy for  $\tau_2$  is much higher [ $E_A(\tau_2) = -58 \text{ kJ/mol}$ ] and in reasonable agreement with  $E_A = -47 \text{ kJ/mol}$  as determined by Wall et al (43) for the second, long-term relaxation in hair. The value is somewhat lower but of the same order as the value determined by Weigmann et al (15) for relaxation through *SH/SS*-interchange ( $-96 \text{ kJ/mol}$ ). Furthermore, it is important to note that neither of the  $\tau_1$  nor the  $\tau_2$ -values shows any indication of the expected transition in the region of 60 - 70 °C, in line with the observations for  $\Delta B_{n1} \& n2$ .

## CONCLUSIONS

Our investigation of the SM-behaviour of perm-waved hair has revealed two underlying viscoelastic recovery processes. Central for our approach to the analysis of the data is the assumption of a fundamental analogy between shape memory from cohesive set on the one hand and from permanent set on the other. Cohesive set and the related shape recovery are based on the breaking and reformation of hydrogen bonds, namely, under the action of water and temperature (3, 21). For this case, the humidity-dependent glass transition of hair is a well-defined and classical ‘trigger’ (8, 10). In the case of permanent set, the *SS*-bonds dynamically form and reform through *SH/SS*-interchange. For this BER, we had reasons (13, 14, 15, 16,

17, 18) to expect the trigger temperature to be around 60 °C in water at neutral pH (16). However, our results show no sign of this transition.

We note that, this transition has generally been observed under conditions of high tensile strains in wool and hair (13, 14, 15, 16, 17, 18, 65). Such strains are well outside the range relevant for perm-wave formation (30, 31). The conspicuous absence of the transition in our results indicates that there is a significant difference between *SH/SS* –driven recovery from low bending strains compared to high tensile strains. This is in line with the differences of the viscoelastic performance of keratin fibres at low strains in the linear viscoelastic (LVE) and at high strains in the non-linear (NLVE) –region, respectively (17, 66).

The main difference between low ( $< 2\%$ ) and higher strains is the degree of  $\alpha \rightarrow \beta$  transition in the helical segments of the IFs (63). The IFs contain in fact only very few *SS*-bonds, namely, in the 2B-segments (63). These segments only unfold at high strains in what is called the post-yield region of hair ( $\epsilon > \approx 30\%$ ) and under special conditions (at higher temperatures in water or under reductive condition) (63). With the absence of the transition at low strains, we hypothesise that the 60 °C transition in water is a BER specific to the *SS* -bonds in the 2B-segments of the IFs at high strains.

In summary, we hypothesise that the shape memory performance of perm-waved hair is dependent on the smooth temperature-dependence of the exchange reactions of covalent bonds in the matrix of the hair composite, considered as autocatalytic, rather than on a well-defined trigger transition. This leads us to classify this behaviour as ‘atypical’.

For the practical context, our investigation explains why a perm-wave may occasionally show unsatisfactory shape formation and stability. This will happen, namely, if hair is not extensively rinsed between processing steps, in line with good hair styling practice (67). We attribute this instability to a higher survival rate of *SH*- or even more reactive *S*<sup>•</sup> -groups, if the internal pH

is not sufficiently re-adjusted towards neutral. The enhanced concentration of SH-groups will facilitate the first, fast SM-process.

For well processed hair the stability of the wave will depend on the 2<sup>nd</sup>, long-term recovery process. If we assume 45 °C as a reasonable upper limit for water temperature for washing hair (12), the mean relaxation time for this process is about 7-8 days. For all practical purposes, the wave will thus be perceived as permanent. Certain life-style habits (e.g., frequent sauna visits: 100 °C,  $\tau_2 \approx 7$  hrs ) may, nevertheless, enhance the consumer perception of hair shape instability.

Against this background, we conclude that the need for re-processing of permed hair after about 6-8 weeks is mainly due to hair re-growths. The additional, perceived loss of shape towards the hair tips is, in our view, not associated with a genuine lack of stability of hair shape or the action of special trigger stimuli (23). We rather attribute it to changes/damage imparted to the morphological structures of the hair through natural weathering processes [a combination of UV-exposure, humidity and heat: (68)] or further common grooming practices [bleaching, dyeing: (69)].

Finally, we are well aware that our decision to neglect certain factors may impose limitations on to the current analysis. First, the assumption of a homogeneous reductive/oxidative treatment is of only limited validity (70, 71), namely, in view of the differences of the accessibility of the disulfide bonds (72). Second, the treatment will impart changes/damage to the IFs as well as the matrix in hair (73, 74). These may, however, be largely compensated due to the structure of Eq. 9. Third, we did not consider a special role for the outer layer of hair, the cuticle (2). It is well known that, the chemical, physical and mechanical properties of the cuticle deviate markedly from those of the cortex (2, 70, 75). Though we maintain that the consistency of our results justify the underlying simplifications and restrictions, we nevertheless believe

that the refinement of the approach may provide substantial academic as well as practically relevant challenges and opportunities for further investigations.

### **CONFLICT OF INTEREST**

The authors declare no conflict of interest.

### **AUTHOR CONTRIBUTIONS**

Conceptualization: FW, GW; Data Organization: CJ, TD; Formal Analysis: FW, TD; Investigation: GW, CJ; Methodology: FW, GW, CJ, TD; Project Administration: FW, CJ; Resources: CJ, TD; Supervision: FW, GW; Visualization: FW; Writing – Original Draft Preparation: FW, GW, CJ, TD; Writing – Review and Editing: FW, GW

### **ACKNOWLEDGEMENT**

We gratefully acknowledge the experimental support by Dr Katie Hardie at the Department of Materials (School of Natural Sciences, University of Manchester, UK).



## References

- 1 Bouillon, C., and J Wilkinson, editors. 2008. *The Science of Hair Care*. 2<sup>nd</sup> edn. Informa Healthcare, New York, London.
- 2 Robbins, C. R. 2012. *Chemical and Physical Behavior of Human Hair*. 5<sup>th</sup> edn. Springer, Berlin, GER.
- 3 Feughelman, M. 1997. *Mechanical Properties and Structure of Alpha-keratin Fibres: Wool, Human Hair and Related Fibres*. UNSW press, Sydney, AUS.
- 4 Powell, B. C., and G.E. Rogers. 1997. The role of keratin proteins and their genes in the growth, structure and properties of hair. In *Formation and Structure of Human Hair*. P. Jolles, H. Zahn, and H. Hoecker, editors. Birkhaeuser, Basel, CH, p.59 – 148.
- 5 Chapman, B. M. 1974. Linear superposition of time-variant viscoelastic responses. *J. Phys. D: Appl. Phys.* 7(17): L185 – 188.
- 6 Denby, E. F. 1975. A note on the interconversion of creep, relaxation and recovery. *Rheol. Acta*. 14(7): 591-593.
- 7 Wortmann, F. J., and S. De Jong. (1985). Analysis of the humidity-time superposition for wool fibers. *Text. Res. J.* 55(12): 750-756.
- 8 Wortmann, F. J., M. Stapels. and L. Chandra. 2009. Humidity-dependent bending recovery and relaxation of human hair. *J. Appl. Polym. Sci.* 113(5): 3336-3344.
- 9 Wortmann, F. J., B.J. Rigby, and D. G. Phillips. 1984. Glass transition temperature of wool as a function of regain. *Text. Res. J.* 54(1): 6-8.
- 10 Wortmann, F. J., M. Stapels, ... , L. Chandra. 2006. The effect of water on the glass transition of human hair. *Biopolymers*. 81(5): 371-375.
- 11 Wickett, R R. 2012 Changing the shape of hair. In *Practical Modern Hair Science*. T. Evans, and R.R. Wickett, editors. Allured Business Media, Carol Stream, IL, USA, Chap 5.
- 12 Feughelman, M. 1990. A note on the permanent setting of human hair. *J. Soc. Cosmet. Chem.* 41: 209-212.
- 13 Feughelman, M. 1966. Sulphydryl–disulphide Interchange and the Stability of Keratin Structure. *Nature*. 211: 1259 - 1260.
- 14 Feughelman, M. 1966. Sulphydryl-Disulfide Interchange in Extended Wool Fibers. *Text. Res. J.* 36(3): 293-294.
- 15 Weigmann, H. D., L. Rebenfeld, and C. Dansizer. 1966. Kinetics and temperature dependence of the chemical stress relaxation of wool fibers. *Text. Res. J.* 36(6): 535-542.

- 
- 16 Chapman, B. M. 1969. A review of the mechanical properties of keratin fibres. *J. Text. Inst.* 60(5): 181-207.
- 17 Yu, Y., W. Yang, and M. A. Meyers. 2017. Viscoelastic properties of  $\alpha$ -keratin fibers in hair. *Acta Biomater.* 64: 15-28.
- 18 Yu, Y., W. Yang, ... , M.A. Meyers. 2017. Structure and mechanical behavior of human hair. *Mater. Sci. Eng. C.* 73: 152-163.
- 19 Weigmann, H. D., L. Rebenfeld, and C. Dansizer. 1965. A transition temperature in wool fibers under stress in relation to structure. *Tex. Res. J.* 35(7): 604-611.
- 20 Millington, K. R., and J.A. Rippon. 2017. Wool as a high-performance fiber. In *Structure and Properties of High-performance Fibers*. G. Bhat, editor. Woodhead Publishing, Duxford, UK, Chap. 14.
- 21 Breakspear, S., B. Noecker, and C. Popescu. 2019. Relevance and Evaluation of Hydrogen and Disulfide Bond Contribution to the Mechanics of Hard  $\alpha$ -Keratin Fibers. *J. Phys. Chem. B.* 123(21): 4505-4511.
- 22 Leng, J., X. Lan, ... , S. Du. 2011. Shape-memory polymers and their composites: stimulus methods and applications. *Prog. Mater. Sci.* 56(7): 1077-1135.
- 23 Xiao, X., J. Hu, ..., K. Qian. 2017. Shape memory investigation of  $\alpha$ -keratin fibers as multi-coupled stimuli of responsive smart materials. *Polymers.* 9(3): 87.
- 24 Ward, I. M., and D. W. Hadley. 1993. *An Introduction to the Mechanical Properties of Solid Polymers*. J. Wiley & Sons Ltd, Chichester, UK.
- 25 Schapery, R. A. 1969. On the characterization of nonlinear viscoelastic materials. *Polymer Engineering & Science.* 9(4): 295-310.
- 26 Boyd, R. H. 1985. Relaxation processes in crystalline polymers: experimental behaviour—a review. *Polymer.* 26(3): 323-347.
- 27 Harper, B. D., and Y. Weitsman. 1985. Characterization method for a class of thermorheologically complex materials. *Journal of Rheology.* 29(1): 49-66.
- 28 Wojtecki, R. J., M.A. Meador, and S. J. Rowan. 2011. Using the dynamic bond to access macroscopically responsive structurally dynamic polymers. *Nature Mater.* 10(1): 14-27.
- 29 Mao, Y., F. Chen, ..., K. Yu. 2019. A viscoelastic model for hydrothermally activated malleable covalent network polymer and its application in shape memory analysis. *J. Mech. Phys. Solids.* 127: 239-265.
- 30 Wortmann, F. J., and I. Souren. 1987. Extensional properties of human hair and permanent waving. *J. Soc. Cosmet. Chem.* 38: 125-140.
- 31 Wortmann, F. J., and N. Kure. 1990. Bending relaxation properties of human hair and permanent waving performance. *J. Soc. Cosmet. Chem.* 41: 123-139

- 
- 32 Wortmann, F. J., M. Stapels, and L. Chandra. 2010. Modeling the time-dependent water wave stability of human hair. *J. Cosmet. Sci.* 61: 31 - 38.
- 33 Robinson, M. S., and B.J. Rigby. 1985. Thiol differences along keratin fibers: stress/strain and stress-relaxation behavior as a function of temperature and extension. *Text. Res. J.* 55(10): 597-600.
- 34 Haly, A. R., and J. W. Snaith. 1967. Differential Thermal Analysis of Wool—The Phase-Transition Endotherm Under Various Conditions. *Text. Res. J.* 37(10): 898-907.
- 35 Feughelman, M., and M. S. Robinson. 1969. Stress Relaxation of Wool Fibers in Water at Extensions in the Hookean Region over the Temperature Range 0°–90° C. *Text. Res. J.* 39(2): 196-198.
- 36 De Jong, S. 1985. Linear viscoelasticity applied to wool setting treatments. *Text. Res. J.* 55(11): 647-653.
- 37 Rebenfeld, L., and C. J. Dansizer. 1963. Mechanical Properties of Set Keratin Fibers. *Text. Res. J.* 33(6): 458-465.
- 38 Hilterhaus-Bong, S. and H. Zahn. 1989. Contributions to the chemistry of human hair: III. Protein chemical aspects of permanent waving treatments. *Int. J. Cosmet. Sci.* 11(5): 221-231.
- 39 Yu, K., Q. Ge, and H. J. Qi. 2014. Reduced time as a unified parameter determining fixity and free recovery of shape memory polymers. *Nature Comm.* 5(1): 1-9.
- 40 Feughelman, M., and F. Irani. 1969. Set in the Hookean and Yield Regions for Wool Fibers. *Text. Res. J.* 39(10): 971-975.
- 41 Haly, A. R., and J. W. Snaith. 1964. Physical Properties of Wool Fibers at Various Regains: Part IX: Further Experiments on Recovery from 20 Percent Extension. *Text. Res. J.* 34(1): 1-5.
- 42 Diaz, P., and M. Y. Wong, M. Y. 1983. Set relaxation of human hair. *J. Soc. Cosmet. Chem.* 34: 205-212.
- 43 Wall, R. A., D.A. Morgan, and G. F. Dasher. 1966. Multiple mechanical relaxation phenomena in human hair. *J. Polym. Sci. C: Polym. Symp.* 14(1): 299-311.
- 44 Sasaki, N., Y. Nakayama, ..., A. Enyo, A. 1993. Stress relaxation function of bone and bone collagen. *J. Biomech.* 26(12): 1369-1376.
- 45 Shirakawa, H., K. Furusawa, ... , N. Sasaki. 2013. Changes in the viscoelastic properties of cortical bone by selective degradation of matrix protein. *J. Biomech.* 46(4): 696-701.
- 46 Verbiest, T., D. M. Burland, and C. A. Walsh. 1996. Use of the lognormal distribution function to describe orientational relaxation in optically nonlinear polymers. *Macromolecules.* 29(19): 6310-6316.

- 
- 47 Angell, C. A., K. L. Ngai, ... , S. W. Martin. 2000. Relaxation in glassforming liquids and amorphous solids. *J. Appl. Phys.* 88(6): 3113-3157.
- 48 Lukichev, A. 2019. Physical meaning of the stretched exponential Kohlrausch function. *Physics Letters A.* 383(24): 2983-2987.
- 49 Struik, L. C. E. 1977. Physical aging in amorphous polymers and other materials. Elsevier Scientific Pub.Co, Amsterdam, NL.
- 50 Chow, T. S. 1992. Glassy state relaxation and deformation in polymers. *Adv. Polym. Sci.* 103: 149-190.
- 51 Rebenfeld, L., H.D. Weigmann, and C. Dansizer. 1966. Temperature dependence of the mechanical properties of human hair in relation to structure. *J. Soc. Cosmet. Chem.* 17: 525-538.
- 52 Tobolsky, A.V. 1971. Viscoelastic Properties of Polymers. In *Polymer Science and Materials*. A. V. Tobolsky, and H. F. Mark, editors. Wiley-Interscience, New York, USA, Chap.10.
- 53 Kadir, M., X. Wang, ... , C. Popescu. 2017. The structure of the “amorphous” matrix of keratins. *J. Struct. Biol.* 198(2): 116-123.
- 54 Pagnotta, S. E., R. Gargana, ... , A. Bocedi. 2005. Glassy behavior of a percolative water-protein system. *Phys. Rev. E.* 71(3): 031506.
- 55 Phillips, J. C. 1994. Microscopic theory of the Kohlrausch relaxation constant  $\beta K$ . *J. Non-cryst. Solids.* 172: 98-103.
- 56 Fancey, K. S. 2001. A latch-based Weibull model for polymeric creep and recovery. *J. Polym. Eng.* 21(6): 489-510.
- 57 Cook, J. R., and B.E. Fleischfresser. 1990. Ultimate tensile properties of normal and modified wool. *Text. Res. J.* 60(1): 42-49.
- 58 Atkins, P. W., and J. De Paula. 2013. *Physikalische Chemie*. Wiley-VCH, Weinheim, GER.
- 59 Wickett, R. R. 1983. Kinetic studies of hair reduction using a single fiber technique. *J Soc Cosmet Chem.* 34: 301-316.
- 60 DiMarzio, E.A. 1986. On the origin of non-exponential decay processes in amorphous solids with application to polymers. In *Transport and Relaxation in Random Materials*. J. Klafter., R.J. Rubin, and M. F. Shlesinger, editors. World Scientific Publishing Company Inc., Maryland, USA, pp. 253 – 277.
- 61 Tomlins, P. E. 1996. Comparison of different functions for modelling the creep and physical ageing effects in plastics. *Polymer.* 37(17): 3907-3913.
- 62 Kubát, J. 1965. Stress relaxation in solids. *Nature.* 205: 378-379.

- 
- 63 Wortmann, F. J., and H. Zahn, H. 1994. The stress/strain curve of  $\alpha$ -keratin fibers and the structure of the intermediate filament. *Text. Res. J.* 64(12): 737-743.
- 64 Feughelman, M., and T. W. Mitchell. 1961. The torsional properties of single wool fibers. Part II. *Text. Res. J.* 31(5): 455-459.
- 65 Feughelman, M., A. R. Haly, and T.W. Mitchell. 1958. The nature of permanent set in keratin fibers. *Text. Res. J.* 28(8): 655-659.
- 66 Wortmann, F. J., and S. De Jong. 1985. Nonlinear viscoelastic behavior of wool fibers in a single step relaxation test. *J. Appl. Polym Sci.* 30(5): 2195-2206.
- 67 Lück, D., and H. Lipp-Thoben. 2013. *Friseurfachkunde*. Springer-Verlag, Berlin, GER.
- 68 Schmidt, H., and F. J. Wortmann. 1994. High pressure differential scanning calorimetry and wet bundle tensile strength of weathered wool. *Text. Res. J.* 64(11): 690-695.
- 69 Wortmann, F. J., G. Wortmann, and C. Popescu. 2019. Linear and nonlinear relations between DSC parameters and elastic moduli for chemically and thermally treated human hair. *J. Thermal Anal. Calorim.* 140: 2171 - 2178.
- 70 Wortmann, F. J., and N. Kure. 1994. Effects of the cuticle on the permanent wave set of human hair. *J. Soc. Cosm. Chem.* 45(3): 149-158.
- 71 Kuzuhara, A., and T. Hori. 2013. Analysis of heterogeneous reaction between reducing agents and keratin fibers using Raman spectroscopy and microspectrophotometry. *J. Molec. Struct.* 1037: 85-92.
- 72 Plowman, J., R. Miller, ... , S. Deb-Choudhury, S. 2021. A detailed mapping of the readily accessible disulfide bonds in the cortex of wool fibers. *Proteins Structure Function and Bioinformatics* DOI:10.1002/prot.26053
- 73 Nishikawa, N., Y. Tanizawa, ..., T. Asakura. 1998. Structural change of keratin protein in human hair by permanent waving treatment. *Polymer.* 39(16): 3835-3840.
- 74 Wortmann, F. J., C. Popescu, and G. Sendelbach. 2008. Effects of reduction on the denaturation kinetics of human hair. *Biopolymers.* 89(7): 600-605.
- 75 Wortmann, F. J., G. Wortmann, ..., W. Eisfeld. 2014. Analysis of the torsional storage modulus of human hair and its relation to hair morphology and cosmetic processing. *J Cosmet Sci.* 65, 59-68.